Alkali Earth Metal Binding Properties of Ionic Microgels

Gary M. Eichenbaum,[†] Patrick F. Kiser,[†,‡] Dipak Shah,[†] William P. Meuer,[§] David Needham,[†] and Sidney A. Simon*,[⊥]

Department of Mechanical Engineering and Materials Science, Duke University, Durham, North Carolina 27708, Access Pharmaceuticals, Dallas, Texas 75207, Division of Earth and Ocean Sciences, Duke University, Durham, North Carolina 27710, and Department of Neurobiology, Duke University Medical Center, Durham, North Carolina 27710

Received October 13, 1999; Revised Manuscript Received March 28, 2000

ABSTRACT: Spherical micron-sized (4−10 μm in diameter) poly(methacrylic acid-*co*-acrylic acid) microgels were synthesized by precipitation polymerization, and their chelation reactions with chloride salts of Mg^{2+}, Ca^{2+}, Sr^{2+}, and Ba^{2+} were investigated by isothermal titration calorimetry (ITC). Ion concentrations obtained by inductively coupled-plasma mass spectrometry (ICP-MS) were used to obtain binding constants and to verify the results obtained by ITC. Although the two methods agreed within 20%, the ITC measurements were experimentally easier to obtain and more accurate. Interference contrast microscopy and micropipet manipulation techniques were used to measure the volume change and corresponding dehydration of the microgels as a function of divalent ion type and concentration. The ITC results showed that the addition of MCl_2 electrolytes, where M represents a divalent metal, with the microgels was an entropy driven reaction in that $\Delta G \sim -20$ kJ/mol $\cong T\Delta S$. These data suggest that the free energy driving the ion exchange (M^{2+} divalent ions for monovalent Na^{+}) is the result of the increase in the entropy of the system; this entropy increase is due to (1) water being "squeezed" from the microgels into the bulk solution and (2) the collapse of the entropy elastic network that accompanies the decrease in the volume of the microgels.

Introduction

Micrometer in diameter ionic hydrogels (microgels) are being explored for use in a number of biomedical applications because of their small size.[1−8] In contrast to centimeter sized ionic hydrogels and ion-exchange resins, their small size permits them to be transported in the bloodstream and even be targeted to certain diseased tissues outside the bloodstream.[9] As a consequence of their high concentration of accessible ionic groups, microgels have the potential to rapidly bind ions from a suspending solution.[7,10] Thus, for biomedical and other applications, in which they may come into contact with different ions and metals, it is important to obtain a fundamental understanding of their ion exchange properties.

Numerous studies of ion binding have been performed on similar, but much larger, ionic macromolecules such as organic ion-exchange resins and ionic hydrogels (also called "slab gels").[11−19] Similarly, a large number of studies have also been performed on the ion binding properties of polyelectrolytes[20] and macromolecules.[21−24] However, to date, there have not been any thermodynamic measurements of the free energy or entropy of ion binding to any ionic slab gels or microgels. This is likely due to the fact that slab gels have significant equilibrium response times (hours to days) that make controlled, ultrasensitive calorimetric measurements difficult. Ionic microgels represent a class of hydrogels that, for the first time in a cross-linked polymer system, can be used to characterize the thermodynamics of ion binding reactions because of their rapid response times (300 ms to reach equilibrium).[7]

In this study our primary goals were to investigate the interactions of microgels with four different sized divalent alkali earth cations (Mg^{2+}, Ca^{2+}, Sr^{2+}, and Ba^{2+}) and then to determine the dependence of these interactions on the radii of the metal cations. To achieve this goal, micron-sized (4−7 μm diameter) poly(methacrylic acid-*co*-acrylic acid) (PMAA) microgels were synthesized by precipitation polymerization. Isothermal titration calorimetry (ITC) was used to measure the solution thermodynamics of the metal complexation reactions with the microgels. An analysis of the thermograms was used to determine the enthalpy, binding constant, and hence free energy and entropy change associated with the binding reactions. To correlate these thermodynamic measurements with a direct measurement on the amount of ions taken up into the microgels, we measured ion concentrations by "inductively coupled plasma mass spectrometry" (ICP-MS). A Langmuir isotherm (single site) model was applied to the ICP-MS results to obtain an independent measure of the equilibrium binding constants associated with the binding reactions. We found that these two methods, based on different physical principles, agreed within experimental error.

To obtain a deeper understanding of the thermodynamic parameters, we used interference microscopy to measure the volume change and corresponding dehydration of a bulk population of microgels as a function of ion concentration.[1,25] We were thereby able to relate, under identical conditions, the enthalpies measured calorimetrically to the degree of dehydration of the microgels. Finally, a micropipet manipulation technique was used to compare the volume condensing effects of protons and monovalent and divalent metals on single

[†] Department of Mechanical Engineering and Materials Science, Duke University.
[‡] Access Pharmaceuticals
[§] Division of Earth and Ocean Sciences, Duke University.
[⊥] Department of Neurobiology, Duke University.
* To whom correspondence should be addressed.

10.1021/ma9917139 CCC: $19.00
Published on Web 04/27/2000

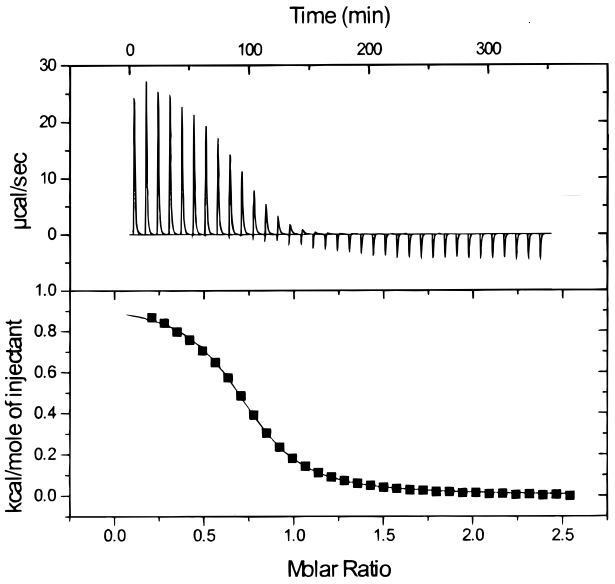

Figure 1. Plot showing the calorimetric titration of the ionic microgels (5 mg/mL) with 35 injections of Ca^{2+} (300 mM) at 298 K in 20 mM PIPES buffer, pH 7.8. The raw data are shown above, and the integrated heats are shown below. The optimal fit to the data gave a binding constant of $K \sim 2.5 \times 10^3$ M^{-1}.

microgels.[7] These data further highlighted the differences in the ion binding mechanisms and provided information on the selectivity of the microgels for different mono- and divalent cations.

Materials and Methods

Poly(methacrylic acid-*co*-acrylic acid) Microgel Synthesis. Poly(methacrylic acid-*co*-acrylic acid) microgels were synthesized by modifying the method developed by Kawaguchi[25,26] and which can be found in Eichenbaum et al.[8] Briefly, the starting materials for the poly(methacrylic acid-*co*-nitrophenyl acrylate) microgels consisted of 4-nitrophenyl acrylate monomer (NPA) (2.07 g), methacrylic acid monomer (MAA) (0.861 g), methylenebisacrylamide cross-linker (MBAM) (0.771 g), azobis(isobutyronitrile) (AIBN) (1.5 g), and ethanol (EtOH) (40 g). The reaction product of the precipitation polymerization was subsequently suspended and then resuspended (four times) in 1 M NaOH (to hydrolyze the nitrophenol groups from the microgels and thus give a random copolymer between acrylic acid, methacrylic acid, and MBAM). To remove the hydrolysis products, the resulting microgel suspension was centrifuged and washed in distilled water four times. Finally, the beads were stored in deionized water at 4 °C.

A copolymerization of methacrylic and acrylic acid is required in order to obtain a monodisperse and homogeneous population of the microgels.[26] The monomer feed ratio for the microgel polymerization consisted of four methacrylic/acrylic acid monomers for every one methylenebisacrylamide cross-linker.

Solution Preparation. To fix the pH at 7.8, all ITC, ICP-MS, and bulk volume experiments were carried out in 10 mM piperazine−*N*,*N*′-bis[2-ethanesulfonic acid] (PIPES) buffer unless otherwise indicated. This pH was selected because it was more than 2 pH units above the apparent pK_a (4.7) of the microgels.[7] This ensured that the ion chelation experiments were a competitive binding between the sodium counterions and the metal ions and did not include protons.

Titration Calorimetry. Experiments were performed with a MCS isothermal titration calorimeter (Microcal, Inc.). Instrumentation and data acquisition/analysis software for an earlier model have been described previously.[27] Solutions were mixed and degassed under vacuum for 10 min to obtain a stable baseline. Experiments were performed at 25 °C. Binding isotherms (Figure 1) were calculated after 35−42 injections from a 101.8 μL injection syringe (containing 300 mM metal ion MCl_2 in pH 7.8, 20 mM PIPES buffer) into a 2.0 mL reaction vessel (containing 10 mg of hydrogels suspended in 20 mM PIPES pH 7.8 buffer). Injection volumes of 3.118 μL (Ca^{2+} and Mg^{2+}) and 4.008 μL (Sr^{2+} and Ba^{2+}) were delivered over 7.84 and 10.08 s intervals, respectively. An interstimulus interval of 200 s allowed for complete equilibration of the solution. Control experiments were performed to correct for the heats of dilution from the injection of the ion/PIPES buffer into the PIPES buffer not containing the microgels (heats of dilution were on the order of −0.4 kJ/mol). For each metal ion the ITC experiments were performed three times. When using the models contained in the data analysis software (Microcal Origin) to curve fit, all parameters (heat of binding, binding constant, and number of binding sites) were allowed to vary.

ICP-MS. For the four divalent alkali earth cations tested, ion binding experiments were carried out using the following procedures. First, a 20 mM stock solution of pH 7.8 PIPES buffer was prepared using distilled deionized water. For each divalent cation, high-purity chloride salts were added to the PIPES buffer to yield 1 mL volumes with ion concentrations that ranged between 0.06 and 9 mM MCl_2. These concentrations matched the range covered in the ITC experiments. The solutions were then divided into two lots, and 1 mg of microgels was added to one lot of the vials containing 1 mL of buffer solution while the other contained no microgels and served as a control. The solutions with microgels were bath sonicated and then incubated for 30 min. Separate experiments revealed that after 30 min no additional uptake was observed. The samples were then centrifuged for 20 min (2500 RCF), and 0.5 mL of supernatant was removed for analysis. To ensure that no microgels were present in the extracted supernatant, the supernatant was filtered through a 100 nm nucleopore filter (Millipore, Inc.). The solutions were then diluted to yield ion-isotope concentrations between 100 ppt and 25 ppb of the isotope(s) to be analyzed for each ion.

Mg^{2+}, Ca^{2+}, Sr^{2+}, and Ba^{2+} concentrations were determined using a VG-Elemental QuadraPole-3 ICP-MS. Machine operating conditions were 1350 W forward power, 0.82 L/min nebulizer flow rate (back-pressure of 35 psi), 0.8−1.0 auxiliary, and 13.5 L/min cool gas flow rates. A concentric-flow nebulizer and double-pass water-cooled spray chamber were used for sample introduction. Analyses are the averages of three 20 s counting periods. A 120 s precontamination (uptake) period was used and a 300 s rinse (using 2% HNO_3). Multiple isotopes for each element were determined to give redundant analyses as follows: ^{25}Mg, ^{26}Mg, ^{43}Ca, ^{44}Ca, ^{86}Sr, ^{87}Sr, ^{135}Ba and ^{137}Ba. A procedural blank was used for blank corrections, and instrument drift was corrected using an external drift monitor. The data were reduced offline using the following algorithm. The raw counts were blank corrected and then drift corrected using linear interpolations between blank solutions and then drift solutions. The corrected counts were then fit to a linear regression defined by the blank and analyses of all control solutions. Analytical uncertainties were less than 3% based on analyses of standard solutions as unknowns.

Volume Response of Microgels to Ion Uptake. a. Bulk Measurements. Images of 50 microgels, suspended in different ionic solutions at different concentrations, were recorded using a camera interfaced with an interference contrast microscope. From measurements of the diameter of the 50 microgels in these images the size distribution was obtained. All bulk diameter measurement data are presented as the mean diameter ± SD.

b. Micropipet Manipulation Measurements. The micropipet flow technique has been described in detail elsewhere.[7] Briefly, the micropipet flow technique, which is centered on an inverted microscope, is a useful method for manipulating and observing the swelling response of individual microgels that have a diameter greater than 1 μm.[7] This technique was used to measure the volume response of the microgels to changes in pH and ionic solution conditions. In a flow pipet experiment, an individual microgel was held by a holding pipet in a chamber, which contained a control solution. Positive pressures (500−1500 N/m^2) were applied to the "flow pipet" (~20 μm i.d.), which was filled with a test solution, by

Table 1. Thermodynamic Parameters for the Binding of Divalent Metals to the Microgels[a]

ion	10^3K (M^{-1})	ΔH (J/mol)	ΔG (kJ/mol)	ΔS (J K^{-1} mol^{-1})	ΔV_{max} (μm^3)*	R_c (A)	R_h (A)
Mg^{2+}	2.4 ± 0.1	870 ± 10	−19.3	69	45	0.72	3.8
Ca^{2+}	3.8 ± 0.5	910 ± 60	−20.4	73	50	0.99	3.6
Sr^{2+}	3.9 ± 0.2	530 ± 30	−20.5	72	58	1.18	3.6
Ba^{2+}	7.8 ± 0.9	350 ± 10	−22.8	77	56	1.35	3.4

[a] Errors are the standard deviations for three ITC runs. ΔV_{max} represents the maximum volume change of the microgels at 9.0 mM for each correesponding divalent metal. R_c is the crystallographic radius,[23] and R_h is the hydrated radius of the metal ion.[37] Note that the volume measurements were not statistically different (*t*-test, $p > 0.05$).

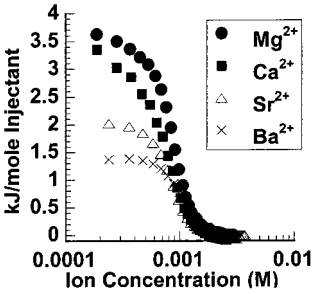

Figure 2. Plot of the integrated heats from the titration of the microgels with four different alkali earth cations.

using a 1 mL syringe acting onto the air gap of a second manometer reservoir. When this flow pipet was aligned axially with the microgel, the microgel became immersed in the flow field of the test solution. For a given set of conditions all micropipet manipulation based measurements were repeated on four different microgels. By using this technique to measure the swelling response of single microgels, the errors associated with diameter measurements of a bulk sample of microgels, as a result of microgel polydispersity, are significantly reduced.[7]

Experimental Results

Thermodynamics of Ion Binding. ITC provides a method for characterizing the thermodynamics of the metal−ligand chelation reactions. A typical plot for the titration of the microgels with Ca^{2+} is shown in Figure 1. Figure 2 shows the integrated heats (of plots similar to the one shown in Figure 1) for the titrations with each of the four alkali earth cations. For all divalent cations, the heat taken up decreased in a sigmoidal fashion and leveled off as the concentration of ions in the bulk solution increased to the point where the binding sites in the microgels became saturated. The heats (ΔH) measured ranged between 350 and 910 J/mol, and the heats increased in the following order: $Ba^{2+} < Sr^{2+} < Mg^{2+} < Ca^{2+}$ (Table 1). The heats for Mg^{2+} and Ca^{2+} were statistically the same but different from those of Ba^{2+} and Sr^{2+}, which were also the same (*t*-test, $p < 0.01$).

By measuring the net change in heat, as a function of the bulk Mg^{2+}, Ca^{2+} (Figure 1), Sr^{2+}, and Ba^{2+} concentrations, we were able to determine each ion-microgel reaction enthalpy (ΔH), apparent binding constant (K_a), reaction free energy ($\Delta G = -RT \ln K_a$), and thereby the reaction entropy (ΔS). To determine the thermodynamic parameters from the heats of reaction shown in Figure 2, we fit a binding curve that assumes one set of noninteracting sites as a first-order approximation.[27] The inputs to the model were the concentration of the ion injection solution, the volume of the injection solution, and the volume of the cell. These were all set experimentally. Good fits were obtained for all of the titration results (average $R^2 = 0.95$). The thermodynamic values obtained by fitting the titration plots for Mg^{2+}, Ca^{2+}, Sr^{2+}, and Ba^{2+} are summarized in Table 1. The binding reactions for all of the ions in the microgels were endothermic and entropy driven (all of the enthalpies and entropies were positive). The entropies varied by only ±5 J K^{-1} mol^{-1}, increasing from 74 to 79 J K^{-1} mol^{-1} for Ca^{2+} and Sr^{2+}, respectively. The binding constants (K_a) and the free energies (ΔG) were in the opposite order from the enthalpies. K_a increased in the following order: $Mg^{2+} < Ca^{2+} < Sr^{2+} < Ba^{2+}$, from 2.4×10^3 M^{-1} for Mg^{2+} to 7.8×10^3 M^{-1} for Ba^{2+}.

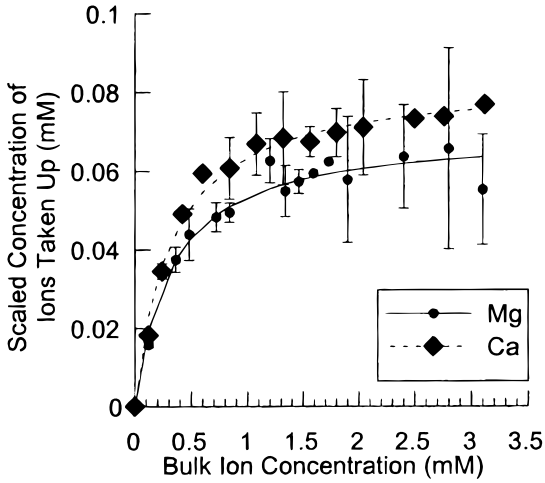

Figure 3. Plot of the scaled concentration of ions taken up into the microgels as a function of the bulk ion concentrations. Scaled concentration refers to the amount of ions taken up divided by the concentration of microgel binding sites in the suspension.

The binding constants for Mg^{2+} and all of the other ions were statistically different (*t*-test, $p < 0.05$). Ca^{2+} and Sr^{2+} were identical but statistically different from Ba^{2+} (*t*-test, $p < 0.05$). Finally, the values of ΔG for the different ions were close in magnitude and ranged from −19.3 to −22.8 kJ/mol for Mg^{2+} and Ba^{2+}, respectively. The free energies were a factor of 1000 larger than the enthalpies and were dominated by the entropy term, $T\Delta S$.

Ion Uptake as a Function of Concentration. Since we used an identical binding site model to calculate K_a by ITC, we sought an independent measure of the binding constants by a more direct technique. Thus, we used ICP-MS to measure the uptake of Mg^{2+} and Ca^{2+} as a function of their bulk concentrations. Figure 3 shows the "scaled concentration" of Mg^{2+} and Ca^{2+} ions taken up into the microgels versus their bulk concentration, where the scaled concentration is the amount of ions taken up divided by the concentration of microgel binding sites. The concentration of binding sites were calculated by bulk titration measurements of the microgels.[7] Comparison of the Mg^{2+} and Ca^{2+} data (Figure 3) indicated that the uptake of the two ions was not statistically different (*F*-test, $\alpha = 0.05$). Note that there was significantly more experimental error associated with this procedure, as compared to ITC (SD =

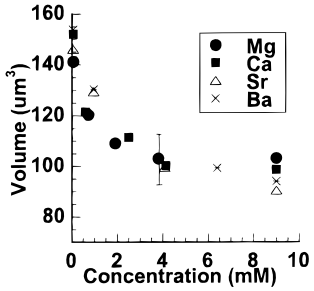

Figure 4. Plot of the average volume of the microgels as a function of the bulk ion concentrations. Note that these data were obtained by measuring the diameters of a somewhat polydisperse population ($n = 50$, SD $\pm$ 0.45 μm) microgels at each ion concentration. This gave rise to significant standard deviations in the measurements.

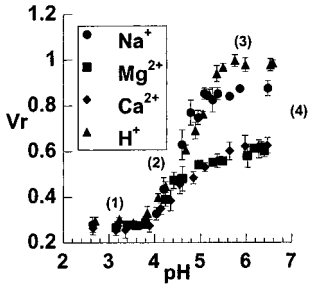

Figure 5. Plot of the microgel equilibrium volume size ratio (V_r) versus pH of the external solution for 10 mM buffer solutions containing no additional ions, 100 mM Na^+, Mg^{2+}, and Ca^{2+}. Error bars on each data point represent the standard deviation of the average swelling ratio of four different microgels. Note that the data contained in this figure were obtained by measuring the volume changes of individual microgels using a micropipet technique. As a result, much smaller measurement errors (1%) than the bulk volume measurements in Figure 4 (10%) were obtained.

$\pm$10% for ITC versus $\pm$30% for ICP-MS). This error was a result of the fact that, as the ion concentration becomes large relative to the amount of ions taken up by the microgels, the initial and final solution concentrations converge. This makes the 3% experimental error by ICP-MS significant.

To obtain the binding constants for Mg^{2+} and Ca^{2+} from the concentration results, we fit the data to a Langmuir adsorption isotherm.[28,29] Excellent fits ($R^2 = 0.99$) were obtained by this method with binding constants, K, of $(3.22 \pm 0.55) \times 10^3$ (SE) M^{-1} for Mg^{2+} and $(3.17 \pm 0.25) \times 10^3$ (SE) M^{-1} for Ca^{2+}. These binding constants were the same, within the standard error, to the binding constants obtained by ITC (2.44×10^3 for Mg^{2+} and 4.02×10^3 for Ca^{2+}). Thus, the ICP-MS results demonstrate that reasonable binding constants can be deduced from ITC results using a relatively simple noninteracting site model. In the Discussion we use the more accurate binding constants obtained by ITC in favor of the binding constants obtained by ICP-MS.

Bulk Volume Response. To directly measure the degree of dehydration associated with the binding reactions, we measured the volume of the microgels as a function of bulk Mg^{2+}, Ca^{2+}, Sr^{2+}, and Ba^{2+} concentrations (Figure 4). The ion concentrations were set at the same levels as those that were used in the ITC experiments. As the ion concentration of the solutions increased from 0.0 to 9.0 mM, the microgel volumes decreased from 148 μm^3 to their minimum volumes of 103, 98, 90, and 92 μm^3 for Mg^{2+}, Ca^{2+}, Sr^{2+}, and Ba^{2+}, respectively (Figure 4). The microgels reached their minimum volume at ion concentrations greater than 3.5 mM (i.e., no statistically significant change in volume was observed between concentrations which were greater than 3.5 mM). This concentration of 3.5 mM was comparable to the scaled concentration at which saturation was reached in the ITC experiments. ANOVA (analysis of variance) indicated that the 13 μm^3 difference in the minimum volumes of the microgels in the strontium solutions as compared to the magnesium solutions (at concentrations = 9.0 mM) was significant ($\alpha = 0.10$, p value < 0.05). The analysis also revealed that there were no other statistically significant ($\alpha = 0.05$, p value < 0.01) volume differences that were detectable between ions at any other concentrations.

Individual Microgel Volume Response. The purpose of measuring volume changes of individual microgels by micropipet manipulation were (1) to provide an accurate basis of comparison for bulk measurements (Figure 4) and (2) to compare the condensing effects of divalent cations to the condensing effects of monovalent sodium ions and protons.[7]. Figure 5 contains a plot of V_r versus pH for microgels that were exposed to 10 mM buffered solutions containing 100 mM Na^+, Ca^{2+}, and Mg^{2+}, with $2Cl^-$ as the counterion and no additional ions. V_r is the ratio of the microgel volume at pHs > 5.3 and specified ion concentration to their maximally swollen volume (in 10 mM buffer). A concentration of 100 mM was chosen for the mono- and divalent ions because it was an order of magnitude greater than the saturation concentration that was used in the bulk measurements. Unlike the bulk volume condensation measurements (Figure 4), where the goal was to compare the volume condensing effects of the different divalent ions in bulk, the goal of micropipet measurements on individual microgels was to compare the condensing effects of protons to those of mono- and divalent ions. Thus, Ca^{2+} and Mg^{2+} were used.

The plot of V_r versus pH for individual microgels (Figure 5) was sigmoidal for all of the solutions. The four major regimes contained in these data were (1) the low-pH regime (pH $\leq$ 3.6), where the swelling of microgels was not affected in a statistically significant manner by either pH or ion concentration (t-test, $p < 0.05$); (2) the pHs of the inflection points, which do not increase significantly (<0.1 pH units) for the different types of ions; (3) the high-pH regime (pH 5.3−6.6) where for a given ion concentration there was a constant value for V_r; and (4) pHs > 5.3, where V_r decreased from 1.0 for protons, to 0.8 in 100 mM Na^+, to 0.6 in 100 mM Ca^{2+} and Mg^{2+}. The volumes of the microgels in the presence of Ca^{2+} and Mg^{2+} were statistically equal (t-test) at all pHs measured.

The micropipet measurements accomplished the first aim of providing a basis of comparison for the bulk volume response measurements. By both methods Ca^{2+} and Mg^{2+} had equivalent condensing effects, and the magnitude of those effects was comparable; V_r was 0.64 by bulk measurements and 0.60 by micropipet manipulation. The second aim of the micropipet measurements, which was to compare the condensation effects and corresponding dehydration of the microgels by monovalent and divalent cations, is discussed in detail below.

Discussion

Thermodynamic Measurements. The results of the ITC measurements (Table 1) showed that for all of the ions the binding and associated volume change of

the microgels was an entropy driven reaction in which $\Delta G \cong T\Delta S \gg \Delta H$. The free energy change in the binding reactions appeared to arise from the entropy gains[30] of both removing water from the microgels[31] and the collapse of the polymer matrix.[32] These increases in entropy due to the binding of divalent counterions are consistent with the thermodynamic observations of divalent ion binding by Williams[30] and are supported experimentally by the volumetric experiments of Strauss et al. using solutions of linear polymers.[20]

For all of the reactions, ΔG was essentially independent of the metal ionic radii (R_c) and instead followed the metal hydrated radii (R_h). Like the free energy, R_h did not change significantly between metal ions (Table 1). With regard to metal selectivity, the microgels were more selective for Ba^{2+} than Mg^{2+}. All other differences in metal selectivity were not statistically significant (*t*-test, $p > 0.05$).

Comparison of the Condensing Effects of Mono- and Divalent Ions. The results of the bulk volume response measurements (Figure 4) showed that there was no statistically significant (*t*-test, $\alpha = 0.05$) difference in the volume change of the microgels between the four different divalent metal ions. In contrast, the results in Figure 5 showed there was a statistically significant difference in the condensing effects of divalent cations as compared to those of monovalent sodium ions and protons. For pHs > 5.3, V_r in the presence 100 mM sodium ions was 0.80 as compared to 0.60 in the presence of 100 mM magnesium and calcium ions. Furthermore, in the presence of 10 mM calcium and magnesium the induced condensation was the same as at 100 mM sodium (Figure 5).[7]

These differences in condensation behavior between sodium and magnesium/calcium were expected on the basis of the differences in their valences (+1 versus +2) and binding affinities for carboxyl groups (10 M^{-1} for sodium[7] as compared to approximately 100 M^{-1} for calcium and magnesium to EDTA[23]). In addition, in contrast to monovalent ions such as sodium, which can only associate or bind to one fixed charge, divalent cations such as calcium have the capability to associate with two fixed charges and can thereby cross-link the polymer network.[11] By cross-linking the polymer chains, divalent ions can bring the chains closer together and dehydrate the microgels to a larger extent than the more weakly bound monovalent ions. However, as discussed below, the cross-linking must occur with partially hydrated divalent cations.

Unlike sodium ions, protons bind more strongly to the microgels than divalent cations. As a result, when the pH becomes more acidic, any counterions in the microgel dissociate and exchange with the protons. For the four curves shown in Figure 5, the exchange of mono- and divalent ions for protons was centered on the microgel apparent pK_a of 4.7[7] and was driven by the fact that protons bind more strongly and completely (i.e., do not remain partially hydrated) to the negative charges on the polymer matrix than any of these cations.[11] In all cases, in the presence of protons (at pHs < 3.6) the microgels collapsed to their minimum volume (V_r = 0.25) independent of the type or concentration of additional counterions present. As was mentioned previously, the difference in the microgel V_r at pHs < 3.6 (V_r = 0.25) versus at pHs > 5.3 in the presence of the divalent ions (V_r = 0.60) suggested that the divalent metal condensed microgels remained more hydrated than the proton condensed microgels.

Table 2. Thermodynamics of Solvation for Metal Ions in Aqueous Solution[23]

ion	$-\Delta G$ (kJ/mol)	$-\Delta H$ (kJ/mol)	$-\Delta S$ (J K^{-1} mol^{-1})
H^+	260.5	269.8	31.3
Na^+	98.3	106.1	35.3
Mg^{2+}	455.5	477.6	74.3
Ca^{2+}	380.8	398.8	60.8
Sr^{2+}	345.9	363.5	59.2
Ba^{2+}	315.1	329.5	48.5

Model To Explain Divalent Metal Binding and Selectivity. To evaluate the factors that determine the microgel divalent alkali earth cation selectivity (Ba^{2+} > Mg^{2+}), we apply a model that was developed by Eisenman[33] that has been successfully used to explain the metal-ion binding selectivity in systems such as glass,[33] crown ethers, and ion selective channels.[34] In the Eisenman model, binding sites range from weak field to strong field. A weak field site is one for which a divalent metal ion of dehydrated radius r_m interacts with an ionic site of dehydrated radius r_s, across a distance r, where r is equal to the sum of r_s, r_m, and the distance of the water layer d_w, having a dielectric constant ϵ. For a given r_m and z_s, where z_s is the valency of the site, weak binding sites will occur when r or r_s is large. This can occur if the charge density of the site is small or if there are water molecules between the ion and the site. For the same metal, a strong field is one in which the small divalent metal ion is completely bound to the site, and there are no water molecules between them.

According to the Eisenman model, the free energies that determine the metal-acid binding equilibrium are $\Delta G_{ion-site}$, the electrostatic free energy of attraction of the metal to the negatively charged site, and $\Delta G_{ion-water}$, the hydration free energy of the metal (eq 1).

$$\Delta G = \Delta G_{ion-site} - \Delta G_{ion-water} \quad (1)$$

Note that the change in free energy from the collapse of the polymer matrix was not considered in the analysis of the microgel metal selectivity because, as shown in Table 1, the microgel volume change was statistically the same for all of the metals (*t*-test, $\alpha = 0.05$).

In the Eisenman model, the binding sites are modeled as spherical ions in a vacuum. From Coulomb's law, the energy (per mole) of interaction ($\Delta G_{ion-site}$) between the sites and naked bound metals (M) depends inversely on the sum of the radii of the ionic site (r_{site}) and the radius of the metal (r_m) (eq 2). For the purposes of applying this model to the microgels, r_{site} is defined as a "virtual site" that is comprised of two carboxyl groups.

$$\Delta G_{ion-site} = \frac{z_{site} z_m e^2 N_B}{4\pi\epsilon\epsilon_0 r} \quad (2)$$

In eq 2, z_{site} and z_m are the valencies of the carboxylic acid and metal ion, respectively, ϵ and ϵ_0 are the relative permittivity and permittivity in a vacuum, respectively, N_B is the number of binding sites per metal ion, and r is the sum of r_s, r_m, and the distance of the water layer d_w. The values for $\Delta G_{ion-water}$ in eq 1 are ion specific and are thus given by the hydration free energies in Table 2.

According to eq 2, the strength of a site is dependent on r_{site} and z_{site}, "weak-field-strength" sites are defined

as those sites for which r and r_{site} are large, and $\Delta G_{ion-site}$ is small relative to $\Delta G_{ion-water}$ for all metals. For weak-field-strength sites, the ion exchange equilibrium (eq 1) is dominated by the dehydration free energies (Table 2) and thus favors binding of larger ions, i.e., $Ba^{2+} > Mg^{2+}$ since the smaller ions are more difficult to dehydrate. Conversely, "strong-field-strength" sites are those for which r and r_{site} are small, and $\Delta G_{ion-site}$ is large relative to $\Delta G_{ion-water}$ for all metals. For strong field sites the ions and sites are in direct contact. For strong-field sites the ion exchange equilibrium is dominated by the ion-site interaction and therefore favors smaller ions, which can draw closest to the attracting carboxylic acid, i.e., $Mg^{2+} > Ba^{2+}$.

We will now show that the experimental results and the Eisenman model suggest that the microgels contain "weak-field" sites that remain partially hydrated when they bind to the metals. The net enthalpies measured by ITC (~−1 kJ/mol) were small compared to the $\Delta H_{solvation}$ for the divalent metals (Table 2, −455.5 kJ/mol for Mg^{2+} to −315.1 kJ/mol for Ba^{2+}), indicating that the divalent metal ions in the microgel were not markedly dehydrated. Further experimental support for this partial hydration comes from the fact that the microgels retained more water when they were completely bound with the divalent metal ions as compared to protons ($V_r = 0.5$ in the presence of metal ions versus $V_r = 0.25$ in the presence of protons). Thus, these results suggest that the microgels did not collapse beyond the hydrated radii of the ions to a point where the crystal radii of the ions would effect the strength and selectivity of association. Finally, the Eisenman model predicts that binding sites in the microgels are weak-field sites that remain partially hydrated, and as such, larger ions such as Ba^{2+} are favored over ions with smaller ionic radii such as Mg^{2+}. These results suggest that weak-field sites not only occur when charge is spread over a high volume but can also occur by virtue of the fact that they are sterically constrained in a high cross-link density microgel.

Comparison of Metal Binding in Linear Ionic Polymers. Previous thermodynamic and volume measurements using linear polyacids provide a useful basis of comparison for these thermodynamic measurements on the microgels. The phase separations that have been observed to occur for linear poly(acrylic acid) and poly(methacrylic acid) solutions in the presence of divalent cations are analogous to the collapse of the microgels.[35] Ewin et al. studied the complexation of alkaline-earth metals by a number of different linear poly(aminocarboxylic) acids such as trimethylenediamine−*N*,*N*′-diacetic acid.[21,22] They found that, like the metal interactions with the microgels, the metal interactions with the linear polymers were also entropy driven ($\Delta G \cong T\Delta S \gg \Delta H$). However, unlike the microgels, the binding constants for these polyacids decreased from 2.5×10^3 M^{-1} for Mg^{2+} to 0.02×10^3 M^{-1} for Ba^{2+}, indicating that the linear polyacids were more selective for Mg^{2+} than Ba^{2+}. According to the Eisenman model (discussed above) this suggests that the binding sites on the linear polymers behave as if they were strong-field-strength sites. It is interesting that despite their difference in selectivity, both systems had very similar binding constants for Mg^{2+}. Although their similarity in binding constants is probably coincidental (this is evident in the difference in entropies and enthalpies discussed below), this result serves to highlight that there is a distinct difference between the ion binding affinity and selectivity of an ionic macromolecule.

The source of the difference in the selectivity of the linear polyacids as compared to the microgels is evident in the different relative reaction entropies and enthalpies of the two systems. The binding enthalpies of the linear polyacids were a factor of 10−100 greater than that of the microgels and unlike the microgels varied significantly between metals, suggesting that the ions were more dehydrated in the linear polymers than in the microgels. The reaction entropies of the linear polyacids were larger than that of the microgels for Mg^{2+} but smaller for Ba^{2+}. In addition, unlike the microgels (Table 1), the reaction entropies of the linear polymers decreased significantly with ionic radius from 99.0 J K^{-1} mol^{-1} for Mg^{2+} to 33.6 J K^{-1} mol^{-1} for Ba^{2+}.

We propose that these differences in the enthalpies, entropies, and selectivity of linear polyacids as compared to the microgels are due to differences in the accessible *configurations of the polymer chains* and therefore *the binding modes* of the metals in both systems.[36] With regard to the polymer configuration, in contrast to the microgels, molecules such as poly(acrylic acid) are single polymer chains. It has been shown previously that nonionized polymers such as poly(acrylic acid) approach a random coil, whereas fully ionized polyacrylic acid is in the form of a winding chain.[32,36] Thus, for the linear polyacids there is significant flexibility for the possible configurations and geometries of the functional groups. In contrast, for the microgels, the proximity of the acid groups is confined to limited separations distances by the highly cross-linked polymer network (5−7 polymer repeat units between cross-links).[8] Thus, in the microgels, steric confinement could prevent the carboxylic acid groups from achieving the same proximity as in a linear polymer. This would result in a fixed common geometry for the functional groups in the microgels and therefore explain their independence of binding on the ionic radius of the metals.

Conclusion

ITC was used to thermodynamically characterize the metal binding reactions of ionic hydrogels. The values that we obtained for the binding constants by ITC were consistent with those obtained by another independent technique, ICP-MS. The results of the ITC experiments showed that the binding of Mg^{2+}, Ca^{2+}, Sr^{2+}, and Ba^{2+} by the microgels was entropically driven and energetically favorable.

The ITC results and application of the Eisenman model suggest that the microgels studied were weak-field-strength sites in which the metals remain partially hydrated upon binding. The fact that they are weak-field-strength sites helped to explain why the microgels were slightly more selective for Ba^{2+} over Mg^{2+}. Differences between the binding and selectivity of ionic microgels as compared to linear polymers suggest that chain mobility may play an important role in determining the selectivity and binding mechanisms in ionic macromolecules. These results also suggest that weak field sites not only occur when charge is spread over a high volume, as was described in the original application of the Eisenman model, but can also occur by virtue of the fact that they are sterically constrained in a high cross-link density microgel.

Acknowledgment. The authors thank Professor Al Crumbliss for helpful discussions. The authors grate-

fully acknowledge financial support from the Duke University Center for Cell and Biosurface Engineering NIH Training Fellowship, North Carolina Space Grant Consortium, Access Pharmaceuticals, NIH-GM 27278, DC 01065 and NIH-GM 40162.

References and Notes

(1) Rembaum, A.; Yen, S.; Cheong, E.; Wallace, S.; Molday, R.; Gordon, I.; Dreyer, W. *Macromolecules* **1976**, *9*, 328−336.
(2) Snowden. *J. Chem. Soc., Chem. Commun.* **1992**, 803.
(3) Urakami, Y.; Kasuya, Y.; Fujimoto, K.; Miyamoto, M.; Kawaguchi, H. *Colloids Surf., B* **1994**, *3*, 183−90.
(4) Achiha, K.; Ojima, R.; Kasuya, Y.; Fujimoto, K.; Kawaguchi, H. *Polym. Adv. Technol.* **1995**, *6*, 534−40.
(5) Kawaguchi, H. *Front. Biomed. Biotechnol.* **1996**, *3*, 157−168.
(6) Kiser, P.; Needham, D.; Wilson, G. *Proc. Am. Chem. Soc.: Div. Polym. Mater. Sci. Eng.* **1997**, *76*, 226.
(7) Eichenbaum, G.; Kiser, P.; Simon, S.; Needham, D. *Macromolecules* **1998**, *31*, 5084−5093.
(8) Eichenbaum, G.; Kiser, P.; Dobrynin, A.; Simon, S.; Needham, D. *Macromolecules* **1999**, *32*, 4867−4878.
(9) Kiser, P.; Wilson, G.; Needham, D. *Nature* **1998**, *394*, 459−462.
(10) Snowden, M.; Thomas, D.; Vincent, B. *Analyst* **1993**, *118*, 1367−1369.
(11) Helfferich, F. *Ion Exchange*; McGraw-Hill Book Company: New York, 1962.
(12) Hasa, J. *J. Polym. Sci., Polym. Phys. Ed.* **1975**, *13*, 263−274.
(13) Hoffman, A. S. Polymeric Biomaterials. In *NATO ASI Series*; Piskin, E. a. H. A. S., Ed.; Martinus Nijhoff Publishers: Dordrecht, The Netherlands, 1986; Vol. 106.
(14) Peppas, N. *Hydrogels in Medicine and Pharmacy;* CRC Press: Boca Raton, FL, 1986; Vol. I.
(15) Kim, S.; Bae, Y.; Okano, T. *Pharm. Res.* **1992**, *9*, 283−290.
(16) Langer, R. *Ann. Biomed. Eng.* **1995**, *23*, 101−111.
(17) Shibayama, M.; Tanaka, T. *Adv. Polym. Sci.* **1993**, *109*, 1−62.
(18) Griffiths, J.; King, J.; Yang, D.; Browner, R.; El-Sayed, M. *J. Phys. Chem.* **1996**, *100*, 929−933.
(19) English, A.; Mafe, S.; Manzanares, J.; Yu, X.; Grosberg, A.; Tanaka, T. *J. Chem. Phys.* **1996**, *104*, 8713−8720.
(20) Strauss, U.; Leung, Y. *J. Am. Chem. Soc.* **1965**, *87*, 1476−1480.
(21) Ewin, G.; Hill, J. *J. Chem. Soc., Dalton Trans.* **1983**, 865−868.
(22) Ewin, G.; Hill, J. *J. Chem. Res. (S)* **1985**, 334−335.
(23) Martell, A.; Hancock, R. *Metal Complexes in Aqueous Solutions*; Plenum Press: New York, 1996.
(24) Albrecht-Gary, A.; Crumbliss, A. Coordination chemistry of siderophores: Thermodynamics and kinetics of iron chelation and release. In *Metal Ions in Biological Systems*; Siegel, A., Siegal, H., Eds.; Marcel Dekker: New York, 1998; Vol. 35, pp 239−327.
(25) Kawaguchi, H.; Kawahara, M.; Yaguchi, N.; Hoshino, F.; Ohtsuka, Y. *Polym. J.* **1988**, *20*, 903−9.
(26) Kashiwabara, M.; Fujimoto, K.; Kawaguchi, H. *Colloid Polym. Sci.* **1995**, *273*, 339−345.
(27) Wiseman, T.; Williston, S.; Brandts, J.; Lung, L. *Anal. Biochem.* **1989**, *179*, 131−137.
(28) Dixon, M.; Webb, E. *Enzymes*; Academic Press: New York, 1960.
(29) Steinhardt, J.; Reynolds, J. *Multiple Equilibria in Proteins*; Academic Press: New York, 1969.
(30) Williams, R. *J. Phys. Chem.* **1954**, *58*, 121−126.
(31) Dunitz, J. *Science* **1994**, *264*, 670.
(32) Flory, P.; Osterheld, J. *J. Phys. Chem* **1954**, *58*, 653−661.
(33) Eisenman, G. *Biophys. J.* **1962**, *2*, 259−323.
(34) Eisenman, G.; Enos, B.; Sandblom, J.; Hagglund, J. *Ann. N.Y. Acad. Sci.* **1980**, *339*, 8−20.
(35) Axelos, M.; Mestdagh, M.; Francois, J. *Macromolecules* **1994**, *27*, 6594−6602.
(36) Jacobson, A. *J. Polym. Sci.* **1962**, *57*, 321−336.
(37) *Aqueous Solutions of Simple Electrolytes*; Franks, F., Ed.; Plenum Press: New York, 1973; Vol. 3.

MA9917139